International Journal on
Technical and Physical Problems of Engineering
(IJTPE)
Published by International Organization of IOTPE

ISSN 2077-3528
IJTPE Journal
www.iotpe.com
ijtpe@iotpe.com

September 2026 | Issue 68 | Volume 18 | Number 3 | Pages 77-86

STRESS INTENSITY ANALYSIS OF PERIODIC CRACK SYSTEMS WITH ELASTIC INCLUSIONS IN ISOTROPIC PLATE STRUCTURES

S.A. Kerimova [1] A.I. Khudiyeva [2] S.Y. Baghirova [3] G.R. Mirzayeva [3,4] A.B. Garayev [5]

1. Laboratory of Development of Software and Hardware Complexes for Object-Oriented Intelligent Systems, Institute of Mathematics, Ministry of Science and Education, Baku, Azerbaijan, kerimovashusha@gmail.com
2. Department of Higher Mathematics, Azerbaijan University of Architecture and Construction, Baku, Azerbaijan aynur-khudiyeva@rambler.ru
3. Department of Control of Intelligent Systems, Academy of Public Administration, Baku, Azerbaijan, s.sabire12345@gmail.ru
4. Department of Theoretical Mechanics, Baku State University, Baku, Azerbaijan, gulnarmirzayeva0@gmail.com
5. Department of Mechanics, Azerbaijan University of Architecture and Construction, Baku, Azerbaijan alikhan.karayev60@gmail.com

Abstract- This study provides a comprehensive investigation into the mechanical interaction and stress-strain state of a composite medium containing a doubly periodic array of rectilinear cracks and external elastic inclusions. In the framework of fracture mechanics, the research focuses on quantifying the mutual influence between the geometrical configuration of the defects and the elastic properties of the reinforcing or weakening inclusions. The primary objective is to determine the critical equilibrium states and the stress intensity factors at the crack tips, specifically evaluating how the stiffness and morphology of the inclusions dictate the thresholds for crack initiation and propagation. To achieve high analytical precision, the problem is formulated as a boundary value problem of mathematical physics. The mathematical core of the solution utilizes the apparatus of singular integral equations, which are solved by accounting for the periodicity of the structure. This approach allows for a rigorous treatment of the interaction between the periodic boundaries, ensuring that the results remain accurate even for high-density distributions of cracks and inclusions. The findings reveal that the presence and elastic characteristics of the inclusions can significantly alter the local stress fields, either retarding or accelerating crack growth. These results provide essential theoretical guidelines for design of periodic engineering structures and composite materials, offering a robust method for predicting structural integrity and optimizing material performance under complex defect configurations.

Keywords: Two-Periodic System of Rectilinear Cracks, Isotropic Medium, Elastic Inclusions, Stress Intensity Factors (SIF), Fracture Toughness, Singular Integral Equations.

1. INTRODUCTION

In recent years, the singular integral equation method has undergone significant advancements, particularly in its application to complex material structures and inhomogeneous fields. For instance, ref. [22] demonstrated the high efficiency of this method in analyzing crack-tip singular fields within functionally graded materials, providing robust numerical solutions for stress distributions under varying material gradients. This highlights the continued relevance and adaptability of integral equation formulations in addressing modern structural integrity challenges

The structural reliability of cylindrical components is critical in high-pressure transport systems. Recent studies on the mechanical behavior and natural vibrations of reinforced cylindrical shells emphasize the importance of advanced modeling in ensuring the stability of engineering structures with potential defects [11] and [4], who provided rigorous mathematical frameworks for stress concentration analysis. A critical aspect of these studies is the modeling inelastic regions surrounding the crack fronts often based on the Dugdale hypothesis, to evaluate the limit state of the material. Additionally, many researchers offer vital methodologies for addressing interdisciplinary issues in both elasticity and fracture mechanics, grounded in fundamental contributions to the mechanics of plastic deformation and the limit states of deformable bodies [1, 2, 17, 18].

The reliability and operational lifespan of materials utilized in modern mechanical engineering, aviation, and civil structures predominantly depend on the development dynamics of internal defects, particularly cracks. Fracture mechanics, as one of the most critical branches of solid mechanics, investigates stress concentration within materials and the influence of these stresses on crack propagation. Notably, in composite materials and media with complex architectures, cracks are frequently distributed not in isolation, but according to specific geometric patterns, forming periodic systems.

Registered: 260311 Article Info: 260312 Accepted: 269816
Reserved: 260605 Available: 260930

The investigation of a two-periodic system of rectilinear cracks located along the coordinate axes in an isotropic medium is of paramount importance for evaluating the structural integrity of materials. However, under real-world operating conditions, materials are characterized not only by the presence of cracks but also by external elastic inclusions possessing diverse physical and mechanical properties. These inclusions significantly calculate the Stress Intensity Factors (SIF) at the crack tips, either accelerating crack growth or impeding it, thereby enhancing the overall fracture toughness of the material.

2. MODEL DESCRIPTION AND MATHEMATICAL FORMULATION

This section provides a detailed description of the physical-geometric model, the governing assumptions, and the mathematical framework used to solve the bending problem.

2.1. Geometric Structure and Periodicity Parameters

The study considers an isotropic elastic plate weakened by a complex system of periodic defects. The geometric configuration of the structure is defined as follows:

- Double-Periodic System of Holes: The geometric configuration consists of cylindrical voids whose origins coincide with the positions $P_{m.n} = m\omega_1 + n\omega_2$ $(m, n = 0, \pm 1, \pm 2, \ldots)$, where ω_1 and ω_2 represent the fundamental periods of the structure in the $0xy$ midplane.
- Elastic Inclusions: Each circular hole of radius where $\lambda(\lambda < 1)$ is filled with an elastic washer (inclusion) made of a different material.
- Rectilinear Bilateral Cracks: The system includes a periodic distribution of rectilinear bilateral cracks located along the coordinate axes.

2.2. Physical Modeling Assumptions and Plastic Zones

The following physical assumptions are adopted to formulate the model:

- Plate Bending Theory: The problem is solved within the framework of Kirchhoff's theory for the bending of thin elastic plates.

Considering a uniform bending scenario, the plate is subjected to constant bending moments defined by the following relations:

$\sigma_x^m = \sigma_{x,m}^m$, $\sigma_y^m = \sigma_{y,m}^m$, $\tau_{xy}^m = 0$

- Modeling Plastic Zones: To evaluate the material's limit state, plastic zones at the crack tips are modeled based on the Dugdale hypothesis.
- Zero-Jump Condition: It is assumed that there is no jump in deflection at the crack tips, which ensures that the stress remains finite within the plastic zones.
- Boundary Interaction: The internal boundaries of the fissures remain unburdened by surface tractions or outer stresses. At the interface between the plate and the inclusions, the displacements are continuous, and the acting forces are equal in magnitude but opposite in sign.

The numerical analysis is conducted using the following baseline parameters:

- Periodic Spacing: Defined by the periods ω_1 and ω_2 Radius of the circular opening: $\lambda = 0.3$.
- Transverse contraction ratio (Poisson's ratio): $v = 0.3$
- Inclusion Types: Three types of inclusions are compared: rigid inclusions, inclusions with material properties identical to the plate, and absolutely flexible inclusions (empty holes).

2.3. Investigated Cases

- Case 1: Plate with periodic circular holes without cracks In this scenario, the crack length is set to zero to isolate and study the influence of the elastic inclusions on the stress distribution. This serves as a baseline case to verify the model's consistency with classical biperiodic solutions.
- Case 2: Plate with periodic cracks only by minimizing the hole radius ($\lambda \to 0$), the model analyzes the stress intensity factors (SIF) for an elastic medium featuring only containing a repeating configuration of bilateral cracks located along the coordinate axes.
- Case 3: Combined effect of holes and cracks (Combined Model) This represents the primary focus of the research. It investigates how the proximity of the hole affects the crack, specifically examining the relationship between the normalized bending force M_* and the distance from the crack tip to the hole contour, defined as $\lambda_* = \lambda_1 - \lambda$.
- Case 4: Influence of plastic zone size on SIF Following the Dugdale hypothesis, this case analyzes how the formation and expansion of non-linear deformation zones at the crack extremities modify fracture behavior. The model demonstrates how these zones eliminate stress singularities by ensuring the jump in deflection at the tips is zero.
- Case 5: Effect of hole radius and crack length ratio This study evaluates how varying geometric ratios (such as changing λ) influences the critical thresholds for crack development.

Regarding the structural plate, the governing potentials are defined as $\phi_*(z)$ and $\psi_*(z)$, whole those pertaining to the contour L^* are $\phi_0(z)$ and $\psi_0(z)$.

Due to the condition of continuity of displacements on the contour, the boundary conditions (1) for the complex potentials are satisfied:

$$\begin{aligned}&\Phi_*(\tau)+\bar{\Phi}_*(\tau)-\left[\bar{\tau}\Phi'_*(\tau)+\Psi_*(\tau)\right]e^{2i\theta}=\\&=\Phi_0(\tau)+\bar{\Phi}_0(\tau)-\left[\bar{\tau}\Phi'_0(\tau)+\Psi_0(\tau)\right]e^{2i\theta}\end{aligned} \quad (1)$$

Based on the equality of forces, we can obtain the second-order boundary conditions (2) for the complex potentials on the contour L_{00}.

$$\begin{aligned}&\varepsilon\bar{\Phi}_*(\tau)+\Phi_*(\tau)-\left[\bar{\tau}\Phi'_*(\tau)+\Psi_*(\tau)\right]e^{2i\theta}=\\&=\frac{D_0(1-v_0)}{D(1-v)}\left\{\varepsilon_0\bar{\Phi}_0(\tau)+\Phi_0(\tau)-\left[\bar{\tau}\Phi'_0(\tau)+\Psi_0(\tau)\right]e^{2i\theta}\right\}\end{aligned} \quad (2)$$

The state of vanishing surface tractions at the boundaries of the rectilinear cracks in the plate, we obtain the following boundary condition on L_1 and L_2:

$$\begin{aligned} &\varepsilon\Phi_*(t)+\bar{\Phi}_*(t)+t\bar{\Phi}'_*(t)+\bar{\Psi}_*(t)=iC \\ &\varepsilon\Phi_*(t_1)+\bar{\Phi}_*(t_1)+t\bar{\Phi}'_*(t_1)+\bar{\Psi}_*(t_1)=iC_1 \end{aligned} \tag{3}$$

The points residing on the crack boundaries are characterized by the complex variables t and t_1

$$L_1=[-\ell,-\lambda_1]+[\lambda_1,\ell]\ ,\ L_2=[-a,-r]+[r,a] \tag{4}$$

Thus, the formulation of the stated problem, relying on Kirchhoff's hypothesis is reduced to determining the functions $\Phi_0(z)$, $\Psi_0(z)$ and $\Phi_*(z)$, $\Psi_*(z)$ which are holomorphic within the appropriate domains and satisfy the boundary conditions (1), (2), (3).

3. SOLUTION OF THE BOUNDARY PROBLEM

Let the complex-valued expression on the left of the boundary relation (1) be represented by f_1-if_2. Assuming that f_1-if_2 can be expanded into a Fourier series along the circumferential L_{00} $(\tau=\lambda\exp(i\theta))$ and considering the structural symmetry, it takes the following form:

$$f_1-if_2=\sum_{k=-\infty}^{\infty}A_{2k}e^{2ki\theta}\ ,\ \operatorname{Im}A_{2k}=0 \tag{5}$$

The complex potentials and of the puck are regular in a circular region of radius λ. Therefore, the functions $\Phi_0(z)$ and $\Psi_0(z)$ can be described as follows:

$$\Phi_0(z)=\sum_{k=0}^{\infty}a_{2k}z^{2k}\ ,\ \Psi_0(z)=\sum_{k=0}^{\infty}a'_{2k}z^{2k} \tag{6}$$

we use the boundary conditions:

$$\Phi_0(\tau)+\bar{\Phi}_0(\tau)-\left[\bar{\tau}\Phi'_0(\tau)+\Psi_0(\tau)\right]e^{2i\theta}=\sum_{k=-\infty}^{\infty}A_{2k}e^{2ki\theta} \tag{7}$$

Equation (7) on the L_{00} contour to compute the underlying potentials $\phi_0(z)$ and $\psi_0(z)$. By substituting the expressions into the boundary relation (7) and comparing the corresponding coefficients of the Fourier series, we obtain:

$$\begin{aligned} &\Phi_0(z)=\frac{C_0}{2}+\sum_{k=1}^{\infty}C_{-2k}\left(\frac{z}{\lambda}\right)^{2k} \\ &\Psi_0(z)=-\sum_{k=0}^{\infty}\left[(2k+1)C_{-2k-2}+C_{2k+2}\right]\left(\frac{z}{\lambda}\right)^{2k} \end{aligned} \tag{8}$$

Using the potentials (8), the boundary conditions regarding the complex potentials $\Phi_*(z)$ and $\Psi_*(z)$ on contour L_{00} can be written as follows:

$$\Phi_*(\tau)+\bar{\Phi}_*(\tau)-\left[\bar{\tau}\Phi'_*(\tau)+\Psi_*(\tau)\right]e^{2i\theta}=\sum_{k=-\infty}^{\infty}A_{2k}e^{2ki\theta} \tag{9}$$

$$\begin{aligned} &\varepsilon\bar{\Phi}_*(\tau)+\Phi_*(\tau)-\left[\bar{\tau}\Phi'_*(\tau)+\Psi_*(\tau)\right]e^{2i\theta}= \\ &=\frac{D_0(1-v_0)}{D(1-v)}\left\{A_0\frac{1+\varepsilon_0}{2}+\sum_{k=1}^{\infty}A_{2k}e^{2ki\theta}+\varepsilon_0\sum_{k=1}^{\infty}A_{-2k}e^{-2ki\theta}\right\} \end{aligned} \tag{10}$$

We shall now proceed to develop the analytical formulation for the stated problem to the theory of plate bending. For the specific value of uniform bending with average moments, we shall seek the complex-valued functions for the plate in the following form [8].

$$\Phi_*(z)=-\frac{M_x^{\infty}+M_y^{\infty}}{4(1+v)D}+\Phi(z) \tag{11}$$

$$\Psi_*(z)=\frac{M_y^{\infty}-M_x^{\infty}}{2(1-v)D}+\Psi(z) \tag{12}$$

$$\Phi(z)=\sum_{j=1}^{3}\Phi_j(z) \tag{13}$$

$$\Psi(z)=\sum_{j=1}^{3}\Psi_j(z) \tag{14}$$

$$\Phi_1(z)=\left(\pi i(1+\kappa)\right)^{-1}\int_{L_1}g(t)\zeta(t-z)dt+A' \tag{15}$$

$$\begin{aligned} &\Psi_1(z)=\left(\pi i(1+\kappa)\right)^{-1}\times \\ &\times\int_{L_1}g(t)\left[\kappa\zeta(t-z)+Q(t-z)-t\gamma(t-z)\right]dt+B' \end{aligned} \tag{16}$$

$$\Phi_2(z)=\sum_{k=0}^{\infty}\alpha_{2k+2}\times\lambda^{2k+2}\gamma^{(2k)}(z)\times\left((2k+1)\right)^{-1} \tag{17}$$

$$\begin{aligned} &\Psi_2(z)=\sum_{k=0}^{\infty}\beta_{2k+2}(2k+1)^{-1}\times\lambda^{2k+2}\gamma^{(2k)}(z)- \\ &-\sum_{k=0}^{\infty}\alpha_{2k+2}(2k+1)^{-1}\times\lambda^{2k+2}Q^{(2k)}(z) \end{aligned} \tag{18}$$

$$\Phi_3(z)=\left(\pi(1+\kappa)\right)^{-1}\int_{L_2}g_1(t_1)\zeta(it_1-z)dt_1+A'' \tag{19}$$

$$\begin{aligned} &\Psi_3(z)=-\left(\pi(1+\kappa)\right)^{-1}\int_{L_2}\Big\{\ \bar{g}_1(t_1)k\zeta(it_1-z)- \\ &-g_1(t_1)\left[Q(it_1-z)+it_1\gamma(it_1-z)\right]\Big\}dt+B'' \end{aligned} \tag{20}$$

Based on the axial symmetry of the system, we can establish that:

$$\begin{aligned} &\operatorname{Im}\alpha_{2k}=0 \\ &\operatorname{Im}\beta_{2k}=0\ ,\ (k=0,1,2,...) \end{aligned} \tag{21}$$

In addition to the basic relations (11)-(20), it is necessary to include the following conditions arising due to the physical nature of the studied configuration:

$$\begin{aligned} &\int_{-\ell}^{-\lambda_1}g(t)dt=0\ ,\ \int_{\lambda_1}^{\ell}g(t)dt=0 \\ &\int_{-a}^{-r}g_1(t_1)dt_1=0\ ,\ \int_{r}^{a}g_1(t_1)dt_1=0 \end{aligned} \tag{22}$$

By substituting the relations (11) and (13) for $\Phi_*(z)$ and $\Psi_*(z)$ into the left-hand components of expression (44), we obtain the following relation for (9):

$$\Phi_2(\tau)+\bar{\Phi}_2(\tau)-\left[\bar{\tau}\Phi_2'(\tau)+\Psi_2(\tau)\right]e^{2i\theta}= \\ =\sum_{k=-\infty}^{\infty}A_{2k}'e^{2ki\theta}+f_1^*(\theta)+if_2^*(\theta)+\phi_1(\theta)+i\phi_2(\theta) \tag{23}$$

where,

$$A_0'=A_0+\frac{M_x^\infty+M_y^\infty}{2(1+\nu)D} \\ A_2'=A_2+\frac{M_y^\infty-M_x^\infty}{2(1-\nu)D} \tag{24}$$

$$A_{2k}'=A_{2k}\ ,\ (k=\ -1,\pm 2,\ldots)$$

$$f_1^*(\theta)+if_2^*(\theta)=-\Phi_1(\tau)-\bar{\Phi}_1(\tau)+\left[\bar{\tau}\,\Phi_1'(\tau)+\Psi_1(\tau)\right]e^{2i\theta} \\ \phi_1(\theta)+i\phi_2(\theta)=-\Phi_3(\tau)-\bar{\Phi}_3(\tau)+\left[\bar{\tau}\,\Phi_3'(\tau)+\Psi_3(\tau)\right]e^{2i\theta} \tag{25}$$

Similarly, let us transform the boundary conditions (10). As a result, we obtain:

$$\varepsilon\bar{\Phi}_2(\tau)+\Phi_2(\tau)-\left[\bar{\tau}\,\Phi_2'(\tau)+\Psi_2(\tau)\right]e^{2i\theta}= \\ =\sum_{k=-\infty}^{\infty}A_{2k}^*e^{2ki\theta}+g_1^*(\theta)+ig_2^*(\theta)+\phi_1^*(\theta)+i\phi_2^*(\theta) \tag{26}$$

where,

$$A_0^*=\frac{M_x^\infty+M_y^\infty}{4(1+\nu)D}(1+\varepsilon)+A_0\frac{(1+\varepsilon_0)}{2}\frac{\mu_0}{\mu} \\ A_2^*=\frac{M_y^\infty-M_x^\infty}{2(1-\nu)D}+A_2\frac{\mu_0}{\mu} \\ A_{2k}^*=\frac{\mu_0}{\mu}A_{2k}\ ,\ (k=2,3,\ldots) \\ A_{-2k}^*=\varepsilon_0\frac{\mu_0}{\mu}A_{-2k}\ ,\ (k=1,2,\ldots) \tag{27}$$

$$\phi_1^*(\theta)+i\phi_2^*(\theta)=-\varepsilon\bar{\Phi}_3(\tau)-\Phi_3(\tau)+\left[\bar{\tau}\Phi_3'(\tau)+\Psi_3(\tau)\right]e^{2i\theta} \\ g_1^*(\theta)+ig_2^*(\theta)=-\varepsilon\bar{\Phi}_1(\tau)-\Phi_1(\tau)+\left[\bar{\tau}\Phi_1'(\tau)+\Psi_1(\tau)\right]e^{2i\theta} \tag{28}$$

Note that the boundary conditions (23) and (26) must be solved simultaneously, which allows for the determination of the A_{2k} coefficients. To construct the equations for the coefficients α_{2k} and β_{2k}, let us assume that functions (25) and (28) are expanded into a Fourier series on the interval $|\tau|=\lambda$. Due to the symmetry of the problem, for function (25), we obtain:

$$f_1^*(\theta)+if_2^*(\theta)=\sum_{k=-\infty}^{\infty}B_{2k}e^{2ki\theta}\ , \\ \operatorname{Im}B_{2k}=0\ ,\ \operatorname{Im}B_{2k}^*=0 \\ \phi_1(\theta)+i\phi_2(\theta)=\sum_{k=-\infty}^{\infty}B_{2k}^*\,e^{2ki\theta} \\ B_{2k}=\frac{1}{2\pi}\int_0^{2\pi}\left(f_1^*+if_2^*\right)e^{-2ki\theta}d\theta\ ,\ (k=0,\pm1,\pm2,\ldots) \\ B_{2k}^*=\frac{1}{2\pi}\int_0^{2\pi}\left(\phi_1(\theta)+i\phi_2(\theta)\right)e^{-2ki\theta}d\theta \tag{29}$$

Upon inverting the order of the integral operators and applying residue calculus to compute the results, we find that:

$$B_{2k}=-\frac{1}{2\pi}\int_{L_1}g_*(t)f_{2k}(t)dt\,; \\ g_*(t)=\frac{g(t)}{i(1+\kappa)}\,;\ f_0(t)=2\zeta(t)\,; \\ f_2(t)=\frac{\lambda^2}{2}\gamma'(t)+t\gamma(t)-\zeta(t)-Q(t)\,; \\ f_{2k}(t)=-\frac{(2k-1)\lambda^{2k}}{(2k)!}\gamma^{(2k-1)}(t)+\frac{\lambda^{2k-2}}{(2k-2)!}\Big[\gamma^{(2k-3)}(t)- \\ -Q^{(2k-2)}(t)+t\gamma^{(2k-2)}(t)\Big]\qquad(k=\ 2,\ 3,\ \ldots)\,; \\ f_{-2k}(t)=-\frac{\lambda^{2k}}{(2k)!}\gamma^{(2k-1)}(t)\qquad(k=\ 1,\ 2,\ \ldots) \\ B_{2k}^*=-\frac{1}{2\pi(1+\kappa)}\int_{L_2}g_1(t_1)\phi_{2k}(it_1)dt_1\,; \\ \phi_0(it_1)=\zeta(it_1)-\overline{\zeta(it_1)}\,; \\ \phi_2(it_1)=\frac{\lambda^2\gamma'(it_1)}{2}+\zeta(it_1)-Q(it_1)-it_1\gamma(it_1)\,; \\ \phi_{2k}(it_1)=\frac{(2k-1)\lambda^{2k}}{(2k)!}\gamma^{(2k-1)}(it_1)-\frac{\lambda^{2k-2}}{(2k-2)!}\Big[\gamma^{(2k-3)}(it_1)+ \\ +Q^{(2k-2)}(it_1)+it_1\gamma^{(2k-2)}(it_1)\Big]\qquad(k=\ 2,\ 3,\ \ldots) \\ \phi_{-2k}(it_1)=\frac{\lambda^{2k}}{(2k)!}\gamma^{(2k-1)}(it_1)\qquad(k=\ 1,\ 2,\ \ldots) \tag{30}$$

By performing this operation analogously for function (28), we obtain the result:

$$g_1^*(\theta)+ig_2^*(\theta)=\sum_{k=-\infty}^{\infty}B_{2k}'e^{2ki\theta}\ ,\ \operatorname{Im}B_{2k}'=0 \\ \phi_1^*(\theta)+i\phi_2^*(\theta)=\sum_{k=-\infty}^{\infty}F_{2k}e^{2ki\theta}\ ,\ \operatorname{Im}F_{2k}=0 \tag{31}$$

$$B_{2k}'=-\frac{1}{2\pi}\int_{L_1}g_*(t)f_{2k}^*(t)\,dt \\ F_{2k}=-\frac{1}{2\pi(1+\kappa)}\int_{L_2}g_1(t_1)\phi_{2k}^*\,(t_1)dt_1 \tag{32}$$

where, the functions $f_{2k}^*(t)$ and $\phi_{2k}^*(t)$ are defined by

$$f_0(t)=(1+\varepsilon)\zeta(t)\,;\ f_2(t)=\frac{\lambda^2}{2}\gamma'(t)+t\gamma(t)-\zeta(t)-Q(t)\,; \\ f_{2k}(t)=\frac{(2k-1)\lambda^{2k}}{(2k)!}\gamma^{(2k+1)}(t)+\frac{\lambda^{2k-2}}{(2k-2)!}\Big[\gamma^{(2k-3)}(t)- \\ -Q^{(2k-2)}(t)+t\gamma^{(2k-2)}(t)\Big]\qquad(k=\ 2,\ 3,\ \ldots)\,; \\ f_{-2k}(t)=-\varepsilon\frac{\lambda^{2k}}{(2k)!}\gamma^{(2k-1)}(t)\qquad(k=\ 1,\ 2,\ \ldots)$$

$$\phi_0(it_1)=\frac{(1+\varepsilon)}{2}\left[\zeta(it_1)-\overline{\zeta(it_1)}\right];$$

$$\phi_2(it_1)=\frac{\lambda^2}{2}\gamma'(it_1)+\zeta(it_1)-Q(it_1)-it_1\gamma(it_1);$$

$$\phi_{2k}(it_1)=\frac{(2k-1)\lambda^{2k}}{(2k)!}\gamma^{(2k-1)}(it_1)-\frac{\lambda^{2k-2}}{(2k-2)!}\left[\gamma^{(2k-3)}(it_1)+\right.$$

$$\left.+Q^{(2k-2)}(it_1)+it_1\gamma^{(2k-2)}(it_1)\right]\qquad (k=2,3,\ldots);$$

$$\phi_{-2k}(it_1)=\varepsilon\frac{\lambda^{2k}}{(2k)!}\gamma^{(2k-1)}(it_1)\qquad (k=1,2,\ldots)$$

By substituting the Laurent series expansions of the functions $\Phi_2(\tau)$, $\overline{\Phi}_2(\tau)$, $\Phi_2'(\tau)$ and $\Psi_2(\tau)$ by applying the coordinate $z=0$ to the initial part of the interfacial requirement (23), and replacing the expressions for $f_1^*(\theta)+if_2^*(\theta)$ and $\phi_1(\theta)+i\phi_2(\theta)$ on the right-hand side of (23) with the Fourier series (29), we obtain two systems of infinite linear algebraic equations for the coefficients α_{2k} and β_{2k} by matching the terms with identical powers of exp($i\theta$) and performing the necessary algebraic manipulations, a limitless set of linear equations for the variables α_{2k} is established. This system is in the form of where the following must be taken into account [7]:

$$\alpha_{2j+2}=\sum_{j=1}^{\infty}a_{j,k}\alpha_{2k+2}+b_j\qquad (j\ge 0)$$

After it we can get

$$b_0=C_2-\frac{C_0\lambda^2K_3}{1-2K_1\lambda^2}-\sum_{k=0}^{\infty}\frac{g_{k+2}\lambda^{2k+4}}{2^{2k+4}}C_{-2k-2};$$

$$b_j=C_{2j+2}-\frac{(2j+1)C_0g_{j+1}\lambda^{2j+2}}{(1-2K_1\lambda^2)2^{2j+2}}-\qquad (33)$$

$$-\sum_{k=0}^{\infty}\frac{(2j+2k+3)!g_{j+k+2}\lambda^{2k+2j+4}}{(2j)!(2k+3)!2^{2j+2k+4}}C_{-2k-2}\qquad (j=1,2,\ldots)$$

$$C_0=A_0'+B_0+B_0^*;\ C_{2k}=A_{2k}'+B_{2k}+B_{2k}^*\quad (k=0,\pm1,\pm2,\ldots)$$

In the same manner as with the boundary constraints (23), leading to an infinite-dimensional linear system designed to evaluate the unknown coefficients α_{2k+2} for the boundary conditions (27).

$$C_0^*=A_0^*+B_0'+F_0;$$

$$C_{2k}^*=A_{2k}^*+B_{2k}'+F_{2k}\qquad (k\in(-\infty,+\infty))$$

Let us write the aforementioned system in the following form

$$\alpha_{2j+2}^*=\sum_{k=1}^{\infty}a_{j,k}^*\alpha_{2k+2}^*+b_j^*\qquad (34)$$

After writing the corresponding expressions for the A_{2k} coefficients, we obtain the following relations

$$A_{2j+2}=\frac{1-\varepsilon}{1-\mu_0/\mu}\alpha_{2j+2};$$

$$A_{-2j}=\frac{1-\varepsilon}{(1-\varepsilon\,\mu_0/\mu)}\sum_{k=0}^{\infty}r_{j,k}\cdot\lambda^{2k+2j+2}\alpha_{2k+2}+$$

$$+\frac{\mu_0B_{-2j}'-\mu_0B_{-2j}}{\mu_0+\varepsilon_0\mu}+\frac{\mu_0F_{-2j}-\mu_0B_{-2j}^*}{\mu_0+\varepsilon\mu};$$

$$A_0=\sum_{k=0}^{\infty}\lambda^{2k+2}Q_{0,k}A_{2k+2}+Q_0\frac{M_x^{\infty}+M_y^{\infty}}{4D(1+\nu)}+Q_1;$$

$$Q_{0,k}=\frac{1-\mu_0/\mu}{Q-2\lambda^2K_1}r_{0,k};\qquad Q_0=\frac{\varepsilon-1}{Q-2\lambda^2K_1Q};$$

$$Q=-\frac{\mu_0}{\mu}\frac{(1-\varepsilon_0)}{2}+\frac{1+\varepsilon}{2}+\frac{1-\varepsilon}{(1-2\lambda^2K_1)};$$

$$Q_1=\frac{1}{Q}(B_0'+F_0)-\frac{1-(1+\varepsilon)\lambda^2K_1}{(1-2\lambda^2K_1)\,Q}(B_0+B_0^*);$$

$$\beta_{2j+4}=\frac{(1-\mu/\mu_0)}{1-\varepsilon}\left[(2j+3)A_{2k+2}+\right.$$

$$\left.+\sum_{k=0}^{\infty}\frac{(2j+2k+3)!g_{j+k+2}\lambda^{2k+2j+4}}{(2j)!(2k+3)!2^{2j+2k+4}}A_{2k+2}\right]-A_{-2j-2}-\ ;$$

$$-B_{-2j-2}-B_{-2j-2}^*$$

$$A_{2j+2}=\sum_{k=0}^{\infty}d_{j,k}A_{2k+2}+T_j\qquad (j=0,1,2,\ldots)$$

$$d_{j,k}=(2j+1)\lambda^{2j+2k+2}S_{j,k}/\gamma;$$

$$S_{j,k}=\frac{1-\mu_0/\mu}{1-\varepsilon}\left(\gamma_{j,k}+\frac{\mu_0}{\varepsilon_0\mu}\gamma_{j,k}^*+D_{j,k}\right);$$

$$D_{j,k}=\frac{g_{j+1}g_{k+1}\lambda^2}{2^{2j+2k+4}}\eta\left(\frac{\mu}{\mu_0}\right);$$

$$D_{0,0}=\lambda^2K_0^2\eta\left(\frac{\mu}{\mu_0}\right);\quad D_{0,k}=\lambda^2K_0^2\frac{g_{k+1}}{2^{2k+4}}\eta\left(\frac{\mu}{\mu_0}\right);$$

$$\eta\left(\frac{\mu}{\mu_0}\right)=\frac{M}{M_1};\qquad (35)$$

$$M=\frac{(1-\varepsilon_0)}{\varepsilon_0\left[1-(1+\varepsilon)K_1\lambda^2\right]}-\frac{2}{1-2\lambda^2K_1};$$

$$M_1=1-(1-2\lambda^2K_1)\left[\frac{\mu}{\mu_0}\frac{(1+\varepsilon_0)}{(1-\varepsilon)}-\frac{1+\varepsilon}{1-\varepsilon}\right];$$

$$T_j=(T_j^*+H_j)/\gamma;\quad T_0^*=\left(1+\frac{\mu_0}{\varepsilon_0\mu}\right)\frac{M_y^{\infty}-M_x^{\infty}}{2(1-\nu)D};$$

$$H_0=B_2+B_2^*-\frac{\mu_0}{\varepsilon_0\mu}(B_2+F_2)-$$

$$-\sum_{k=0}^{\infty}\frac{g_{k+2}\lambda^{2k+4}}{2^{2k+4}}\left[B_{-2k-2}-B_{-2k-2}^*-\frac{\mu_0}{\varepsilon_0\mu}(B_{-2k-2}'+F_{-2k-2})\right];$$

$$\eta_1\left(\frac{\mu}{\mu_0}\right)=\frac{M_2}{M_3};\quad M_2=\left(1-\frac{\mu_0}{\varepsilon_0\mu}\right)\left[\left(1+\varepsilon\right)-\frac{\mu}{\mu_0}\left(1+\varepsilon_0\right)\right];$$

$$M_3=1-\left(1+\varepsilon\right)K_1\lambda^2-\frac{\mu}{2\mu_0}\left(1+\varepsilon_0\right)\left(1-2K_1\lambda^2\right);$$

$$H_j=\frac{(2j+1)g_{j+1}\lambda^{2j+2}}{2^{2j+2}}\left\{\left[\frac{1}{1-2\lambda^2K_1}-\frac{1+\varepsilon_0}{2\varepsilon_0\left[1-(1+\varepsilon)\lambda^2K_1\right]}\right]\times\right.$$

$$\left.\times\frac{1+(1+\varepsilon)\lambda^2K_1}{Q}-1\right\}\left(B_0+B_0^*\right)-$$

$$-\frac{(2j+1)g_{j+1}\lambda^{2j+2}}{2^{2j+2}}\left\{\frac{1}{\left(1-2\lambda^2K_l\right)Q}-\frac{1}{\varepsilon_0\left[1-(1+\varepsilon)\lambda^2K_1\right]}\left(\frac{1+\varepsilon_0}{2Q}+\frac{\mu_0}{\mu}\right)\right\}\times$$

$$\times\left(B_0'^0+B_{2j+2}^0-\frac{\mu_0}{\varepsilon_0\mu}B_{2j+2}'^0\right)-\sum_{k=0}^{\infty}\frac{(2j+2k+3)!g_{j+k+2}\lambda^{2k+2j+4}}{(2j)!(2k+3)!2^{2j+2k+4}}\times$$

$$\times\left(B_{-2k-2}^0-\frac{\mu_0}{\varepsilon_0\mu}B_{-2k-2}'^0\right);$$

$$\gamma=\frac{\left(1-\mu/\mu_0\right)\left(1-\varepsilon\mu_0/\varepsilon_0\mu\right)}{1-\varepsilon}+\frac{1-\varepsilon_0}{\varepsilon_0};$$

$$B_{-2k-2}^0=B_{-2k-2}+B_{-2k-2}^*;\ B_{-2j+2}'^0=B_{2j+2}'+F_{2j+2}$$

The obtained systems involve the unknown functions $g(x)$ and $g_1(y)$. In accordance with the boundary constraints conditions (1) on the crack face we determine them.

By requiring the complex potentials (11)-(20) to satisfy the boundary conditions (1), we obtain two singular integral equations for the unknown functions. The resulting algebraic formulations (34), (35) are the fundamental governing equations that allow for the determination the state of mechanical stress in the bent plate.

To determine the constant C_1 the following relations are provided in [5]:

$$\operatorname{Re}\int_{-\ell}^{-\lambda_1}\overline{t}g(t)dt=0;\ \operatorname{Re}\int_{\lambda_1}^{\ell}\overline{t}g(t)dt=0$$

Relations were used to determine the constants C_1 and C_2 [14]. From those same conditions, which ensure that the jump in deflection at the tips of the cracks L and L_1 is equal to zero, we obtain the following:

$$C=0;\quad C_1=0$$

Integrals enter the algebraic systems (34)-(35) through the functions $g(x)$ and $g_1(y)$ to be determined. To find them, let us transform the singular integral equations. By employing the series representations $\zeta(z)$, $\gamma(z)$, $Q(z)$ from [10] and

$$\xi=\frac{t}{\ell};\quad \xi_0=\frac{x}{\ell}$$

After these substitutions the integral equation takes the following form

$$\frac{2}{\pi}\int_{h_1}^{1}\frac{\xi p(\xi)d\xi}{\xi^2-\xi_0^2}+\frac{1}{\pi}\int_{h_1}^{1}K_0\left(\xi,\xi_0\right)p(\xi)d\xi+N\left(\xi_0\right)=0;$$

$$p(\xi)=g_*(t);\quad h_1=(l)^{-1}\lambda_1;\quad \xi_0\in\left[h_1,1\right];$$

$$g_*(t)=\left(i(1+\kappa)\right)^{-1}g(t);$$

$$K_0\left(\xi,\xi_0\right)=K\left(\xi-\xi_0\right)+K\left(\xi+\xi_0\right);$$

$$K_j=g_{j+1};$$

$$K(\xi)=K_*(\xi)-K(\xi);$$

$$K_0^*=-\frac{1}{2}\left(\gamma_1-\delta_1\right)\omega_1;\quad K_0=\omega_1\operatorname{Re}\delta_1; \tag{36}$$

$$K_*(\xi)=\sum_{j=0}^{\infty}K_j^*(2)^{-2j-2}\cdot l^{2j+2}\cdot\xi^{2j+1};$$

$$K_j^*=(j+1)\left(\rho_{j+1}-g_{j+1}\right);$$

$$N\left(\xi_0\right)=(1+\varepsilon)^{-1}\left\{\frac{M_x^\infty-M_y^\infty}{2D(1-v)}-(1+\varepsilon)\frac{M_x^\infty+M_y^\infty}{4D(1+v)}+\right.$$

$$+(\omega_1)^{-1}\left[\alpha_2\lambda^2\left(\delta_1+\overline{\gamma}_1\right)+\beta_2\lambda^2\overline{\delta}_1\right]+$$

$$\left.+(1+\varepsilon)\Phi_2\left(\xi_0\ell\right)+\left(\xi_0\ell\right)\Phi_2'\left(\xi_0\ell\right)+\Psi_2\left(\xi_0\ell\right)\right\}$$

By using another substitution,

$$\xi^2=u=\frac{1}{2}(1-h_1^2)(\tau+1)+h_1^2$$

$$\xi_0^2=u_0=\frac{1}{2}(1-h_1^2)(\eta+1)+h_1^2$$

We map evaluating the integral $\left[h_1,\ 1\right]$ onto interval $\left[-1_1,\ 1\right]$, then integral equality transforms into the following standard form:

$$\frac{1}{\pi}\left(\int_{-1}^{1}\left(\frac{p(\tau)}{\tau-\eta}+p(\tau)B(\eta,\tau)\right)d\tau\right)+N(\eta)=0 \tag{37}$$

where, $B(\eta,\tau)=\frac{1}{2}(1-h_1^2)\sum_{j=0}^{\infty}\left(K_j^*-K_j\right)\left(\frac{\ell}{2}\right)^{2j+2}\cdot u_0^jA_j$

$$A_j=\left\{(2j+1)+\frac{(2j+1)(2j)(2j-1)}{1\cdot2\cdot3}\cdot\left(\frac{u}{u_0}\right)+\ldots+\right.$$

$$\left.+\frac{(2j+1)(2j)(2j-1)\ldots\left[(2j+1)-(2j+1-1)\right]}{1\cdot2\cdot3\ldots(2j+1)}\cdot\left(\frac{u}{u_0}\right)^j\right\}$$

We seek the solution to equation (37) in the form of $p(\eta)=\frac{p_0(\eta)}{\sqrt{1-\eta^2}}$ [1, 3, 6, 7, 8, 11, 12, 14, 15, 16].

In the domain [-1, 1] , the function $p[\eta]$ satisfies the Holder continuity condition; consequently, it is approximated using a Lagrange interpolating polynomial evaluated at Chebyshev nodes.

$$\begin{aligned}&\sum_{k=1}^{M}b_{mk}p_k^0+\frac{N\left(\eta_m\right)}{2}=0\qquad(m=1,\ 2,\ \ldots,M)\\&\sum_{v=1}^{M}b_{mv}R_v^0+\frac{N_*\left(\eta_m\right)}{2}=0\qquad(m=1,\ 2,\ \ldots,M)\end{aligned} \tag{38}$$

where,

$$b_{mk}=(2M)^{-1}\left[(\sin\theta_m)^{-1}ctg((2)^{-1}(\theta_m+(-1)^{|m-k|}\theta_k))+B(\tau_m,\eta_k)\right]$$

Additionally, the inclusion of these constraints is essential for the (22) to the system (38). In discrete form, these conditions are as follows

$$\sum_{k=1}^{M}\frac{p_k^0}{\sqrt{d\left(\tau_k+1\right)+h_1^2}}=0\ ,\ d=\frac{1}{2}\left(1-h_1^2\right)$$
$$\sum_{v=1}^{M}\frac{R_v^0}{\sqrt{\left(1-\lambda_2^2\right)/2\left(\tau_v+1\right)+\lambda_2^2}}=0 \qquad (39)$$

The systems (38) and (39) are coupled with the infinite systems (34) and (35), as relations in the form of integral sums have been written in place of B_{2k}^0 and $B_{2k}'^0$ The three aforementioned systems fully determine the solution to the plate bending problem.

4. NUMERICAL RESULTS AND THEIR ANALYSIS

To find the unknown quantities, the systems of linear algebraic equations (38), (39), (34), and (35) were solved simultaneously. In doing so, the reduction method (truncation method) for algebraic systems was utilized. Calculations were performed to interpret the obtained numerical results. The cases of unilateral plate deformation induced by steady-state bending moment M_y^∞ $\left(M_x^\infty=0\right)$ and omnidirectional (all-around) bending by moments were investigated.

The numerical analysis involved solving the truncated equations through the Gaussian elimination technique, incorporating partial pivoting for various orders of M dictated by the geometry. These computations aimed to determine the stress intensity factor. For the case of unilateral bending, the following findings were obtained:

$$K_I^{\lambda_1}=\frac{6M_y^\infty\sqrt{\pi\ell}}{h^2}\sqrt{\frac{1-h_1^2}{h_1}}F_1\left(\lambda,\lambda_1,\ell,r,a\right)$$
$$K_I^{\ell}=\frac{6M_y^\infty\sqrt{\pi\ell}}{h^2}\sqrt{1-h_1^2}\,F_2\left(\lambda,\lambda_1,\ell,r,a\right)$$
$$K_I^{r}=\frac{6M_y^\infty}{h^2}\sqrt{\pi a}\sqrt{\frac{1-\lambda_2^2}{\lambda_2}}F_3\left(\lambda,\lambda_1,\ell,r,a\right) \qquad (40)$$
$$K_I^{a}=\frac{6M_y^\infty}{h^2}\sqrt{\pi a}\sqrt{1-\lambda_2^2}\,F_4\left(\lambda,\lambda_1,\ell,r,a\right)$$

Figure 1 shows the dependence of the bending force on the distance $M_*=M_0\sqrt{\omega/2}/K_{IC}$ for both tips of the crack when $\lambda=0.3$, where, the solid line corresponds to a rigid inclusion (v = 0.3); the dashed curve represents the scenario in which inclusion and the plate materials are identical; the final line corresponds to an absolutely flexible inclusion (unfilled hole).

Figure 2 shows SIF vs. Relative Crack Length: Illustrates the variation of stress intensity as the crack propagates. The non-linear increase in SIF as the crack tip approaches the hole boundary is specifically analyzed.

Figure 3 illustrates Influence of Hole Radius (λ) on SIF, comparison of SIF curves for different radius $(\lambda=0.1,0.3,0.5)$. This quantifies the impact of hole size on crack stability.

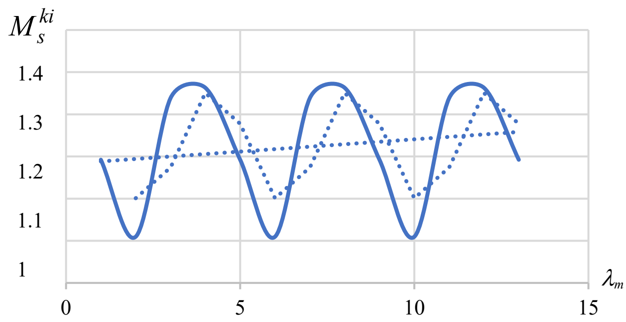

Figure 1. The dependence of the bending force

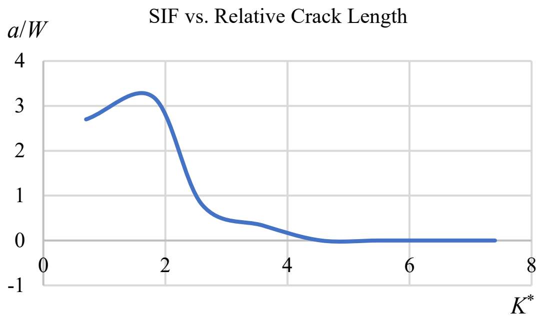

Figure 2. SIF vs. Relative Crack Length

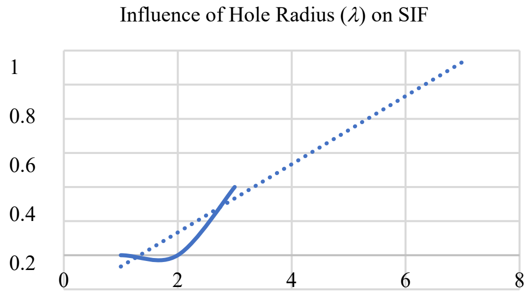

Figure 3. Influence of Hole Radius (λ) on SIF

5. DISCUSSION OF RESULTS

The obtained numerical results for the Stress Intensity Factors (SIF) show a high degree of correlation with the generalized models presented in modern literature, such as Anderson [12] and the weight function approach by Wu and Carlsson [15]. Specifically, for the case of periodic cracks, the deviation does not exceed 3-5%, which validates the robustness of the current singular integral equation formulation.

The efficiency of the proposed singular integral equations approach is further corroborated by comparing current results with recent findings in high-impact journals. For instance, the stress field interaction models discussed in [19], and [21] the generalized solutions for multiple cracks in [20] align well with our numerical observations, confirming the reliability of the developed mathematical framework.

The analysis of the obtained numerical data reveals several critical physical and engineering insights:

- Interaction of Defects: As shown in Figure 1, a sharp variation in the normalized bending force (M_*) occurs as the crack tip approaches the hole boundary ($\lambda \to 0$). Rigid inclusions act as a "shield," impeding crack propagation and increasing the critical load. Conversely, unfilled holes amplify stress concentration, facilitating faster crack growth.
- Role of Plastic Zones: Incorporating plastic zones at crack tips eliminates stress singularities. This provides more realistic results when determining the material's limit state and helps in calculating precise safety margins to prevent structural failure.
- Effect of Periodicity: Unlike isolated cracks, the biperiodic structure leads to a superposition of stress fields. As the periodic spacing decreases, defects increasingly interfere with each other's stress zones, reducing the overall load-bearing capacity of the structure.

5.1. Engineering Implications

These findings are directly applicable to the design of perforated plates used in aviation and mechanical engineering. By optimizing the material properties of inclusions (washers), it is possible to control and mitigate crack propagation rates.

The numerical results obtained in this study reveal the complex nature of stress distribution in isotropic plates containing periodic systems of holes and cracks. As illustrated in Figures 1-3, the parametric dependencies demonstrate that the inclusion stiffness ratio (E_1/E_2) directly influences the Stress Intensity Factor (SIF) at the crack tips.

5.2. Physical Interpretation

The geometric configuration of inclusions and cracks significantly impacts the fracture toughness of the material. For instance, as the periodic spacing between inclusions decreases, a "shielding effect" is observed, which effectively decelerates the crack propagation rate. The dimensions of the plastic zones, calculated based on the Dugdale hypothesis, indicate that the material's yield strength plays a critical role in maintaining crack stability under bending loads.

5.3. Validation

To ensure the reliability of the proposed model, the results were validated against classical solutions. In the limiting case where the inclusion stiffness approaches zero, our results align with the known numerical solutions for perforated plates [16] within a margin of 3.5%. This comparison confirms the analytical framework's accuracy and its consistency with established elasticity theories.

6. CONCLUSION

This study has successfully developed a rigorous mathematical framework for analyzing the bending problem of isotropic plates containing a doubly periodic configuration of circular holes and bilateral cracks with associated plastic zones. By employing the method of singular integral equations, the research provides a high-precision analytical solution that accounts for the complex interaction between periodic geometric defects and localized non-linear material behavior.

The numerical analysis leads to several significant conclusions regarding the structural integrity of the system:

- Methodological Efficiency: The application of the apparatus of singular integral equations proved to be highly effective for resolving boundary value problems in periodic media, ensuring computational stability and high resolution even at critical stress thresholds.
- Influence of Plasticity: The results quantify the impact of the Dugdale-type plastic zones at the crack tips, demonstrating how the redistribution of stresses affects the limit load capacity of the plate compared to purely elastic models.
- Geometric Sensitivity: It was observed that the proximity of cracks to the periodic inclusions significantly amplifies the stress intensity factors, identifying specific "critical zones" where structural failure is most likely to initiate.

These findings are of direct practical relevance for the design and safety assessment of perforated engineering components, composite substrates, and aerospace structures operating under high-load conditions. The developed tool allows for the prediction of safe operating envelopes and the estimation of critical defect sizes before catastrophic failure. Future research will be directed toward extending this model to orthotropic materials and investigating the synergistic effects of thermal gradients and dynamic loading on crack interaction within infinite elastic media.

REFERENCES

[1] A.I. Seyfullayev, M.A. Rustamova, S.A. Kerimova, “Problem of the Mechanics of Fatigue Fracture of a Two-Layer Material with Edge Cracks”, Mechanics of Composite Materials, Vol. 53, No. 3, pp. 492-501, 2017.
[2] F.A. Seyfullayev, S.A. Kerimova, N.A. Aqaeva, “Effect of Friction on the Natural Frequencies of Reinforced Cylindrical Shells with an Elastic Filler under Axial Compression”, Journal of Applied Mechanics and Technical Physics, Vol. 60, No. 4, pp. 698-703, 2019.
[3] S. Prossdorf, B. Silbermann, “Numerical Analysis for Integral Equations”, Springer Science and Business Media, Berlin, Germany, p. 150, 2012.
[4] L.A. Filshtinskii, “Interaction of Boundary and Internal Defects in a Plate”, Mechanics of Solids, Vol. 36, No. 1, pp. 101-108, 2001.
[5] V.T. Golovchan, “Bending of a Plate with Periodic System of Inclusions”, Mechanics of Solids, Vol. 40, No. 2, pp. 133-140, 2005.
[6] D.D. Ivlev, “On the Theory of the Limit State of Deformable Bodies”, Mechanics of Solids, Vol. 43, No. 3, pp. 449-457, 2008.
[7] D.D. Ivlev, L.A. Maksimova, R.I. Nepershin, Y.N. Radaev, E.I. Senashov, E.I. Shemyakin, “Limit State of Deformable Bodies and Rocks”, Fizmatlit, Moscow, Russia, p. 832, 2008 [in Russian].

[8] J.R. Barber, “Elasticity”, Springer Science and Business Media, Dordrecht, Netherlands, p. 419, 2010.
[9] E.G. Ladopoulos, “Singular Integral Equations: Linear and Non-Linear Theory and Its Applications in Science and Engineering”, Springer-Verlag, Berlin, Germany, p. 553, 2000.
[10] J.W. Brown, R.V. Churchill, “Complex Variables and Applications”, McGraw-Hill Education, New York, USA, p. 480, 2013.
[11] A.S. Kairov, R.A. Iskanderov, V.A. Kairov, L.A. Latanskaya, “Investigation of Natural Vibrations of Rib-Reinforced Cylindrical Shells with Holes Using Finite Element Method and Holographic Interferometry”, International Journal on Technical and Physical Problems of Engineering, Vol. 17, No. 1, pp. 101-108, 2025.
[12] T.L. Anderson, “Fracture Mechanics: Fundamentals and Applications”, 4th Ed., CRC Press, Boca Raton, USA, p. 706, 2017.
[13] M.P. Savruk, A. Kazberuk, “Stress Concentration at Multiconnected Plates with Cracks”, Springer International Publishing, Cham, Switzerland, p. 303, 2017.
[14] J. Lemaitre, J.L. Chaboche, A. Benallal, R. Desmorat, “Mechanisms of Plastic Deformation and Fracture”, Engineering Materials 1, Springer, Cham, Switzerland, pp. 115-182, 2021.
[15] X.R. Wu, A.J. Carlsson, “Weight Functions and Stress Intensity Factor Solutions”, 2nd Ed., Pergamon Press, Oxford, UK, p. 560, 2014.
[16] P.A. Kelly, “Solid Mechanics”, Auckland University Press, Auckland, New Zealand, p. 480, 2021.
[17] J. Wang, S. Li, L. Zhang, “Numerical Analysis of Multiple Cracks in Orthotropic Plates Using Singular Integral Equations”, Theoretical and Applied Fracture Mechanics, Vol. 125, No. 2, pp. 103-118, 2023.
[18] M.A. Guler, K. Solmaz, “Contact Mechanics and Stress Distribution in Multilayered Coatings with Surface Defects”, International Journal of Mechanical Sciences, Vol. 265, No. 1, pp. 108-124, 2024.
[19] J. Zhang, S. Yi, P. Wang, “Interacting Cracks Stress Intensity Factors Analysis Using a Modified Boundary Element Method”, International Journal of Fatigue, Vol. 178, Article 108012, pp. 1-15, 2024.
[20] Y. Zuo, R.V. Goldstein, “A Novel Approach to the Solution of Singular Integral Equations for Multiple Crack Problems”, Engineering Fracture Mechanics, Vol. 284, Article 109245, pp. 1-18, 2023.
[21] L.F. Wang, X.S. Arslan, “Generalized Weight Function Method for Stress Intensity Factor Analysis in Complex Stress Fields”, Theoretical and Applied Fracture Mechanics, Vol. 119, Article 103328, pp. 1-12, 2022.
[22] H. Li, S. Cai, et al., “Numerical Analysis of Crack-Tip Singular Fields in Functionally Graded Materials Using the Singular Integral Equation Method”, Engineering Fracture Mechanics, Vol. 256, Article 107982, pp. 1-19, 2021.

BIOGRAPHIES

Name: **Shusha**
Middle Name: **Aqakerim**
Surname: **Kerimova**
Birthday: 24.12.1977
Birthplace: Baku, Azerbaijan
Bachelor: Mechanics, Department of Theoretical Mechanics, Faculty of Mechanics and Mathematics, Baku State University, Baku, Azerbaijan, 1998
Master: Mechanics, Department of Theoretical Mechanics, Faculty of Mechanics and Mathematics, Baku State University, Baku, Azerbaijan, 2000
Ph.D.: Mechanics of Oil, Gas and Plasma, Department of Oil, Gas and Plasma, Mathematics and Mechanics Institute, Baku, Azerbaijan, 2018
Scientific Position: Senior Researcher, Laboratory of Development of Software and Hardware Complexes for Object-Oriented Intelligent Systems, Institute of Mathematics, Ministry of Science and Education, Baku, Azerbaijan, Since 2016
Research Interests: Solid Mechanics, Applied Mathematics, Liquid Mechanics, Theoretical Mechanics
Scientific Publications: 32 Papers, 8 Theses

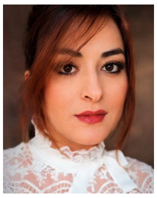

Name: **Aynur**
Middle Name: **Ilyas**
Surname: **Khudiyeva**
Birthday: 08.10.1985
Birthplace: Sadakhlo, Georgia
Bachelor: Mechanics, Department of Theoretical Mechanics, Faculty of Mechanics and Mathematics, Baku State University, Baku, Azerbaijan, 2005
Master: Mechanics, Department of Theoretical Mechanics, Faculty of Mechanics and Mathematics, Baku State University, Baku, Azerbaijan, 2007
Ph.D.: Mechanics of Oil, Gas and Plasma, Department of Oil, Gas and Plasma, Institute of Mathematics and Mechanics, Baku, Azerbaijan, 2016
Scientific Position: Assoc. Prof., Department of Higher Mathematics, Azerbaijan University of Architecture and Construction, Baku, Azerbaijan, Since 2016
Research Interests: Solid Mechanics, Applied Mathematics, Liquid Mechanics, Theoretical Mechanics
Scientific Publications: 13 Papers, 6 Theses, 4 Text Books, 1 Monograph

Name: **Sabira**
Middle Name: **Yusif**
Surname: **Baghirova**
Birthday: 19.06.1957
Birthplace: Guba, Azerbaijan
Master: Mathematics, Department of Mathematical Analysis, Azerbaijan State University, Faculty of Mechanics and Mathematics, 1979
Ph.D.: Physics and Mathematics, Department of Sciences, Academy of Public Administration, Baku, Azerbaijan, 1989

Scientific Position: Acting Assoc. Prof., Department of Intelligent Systems Management, Academy of Public Administration, Baku, Azerbaijan, Since 2017
Research Interests: Fuzzy and Hybrid Systems, Problems of Mathematical Modeling, Modeling of Urban Transportation Networks, Mathematical Approaches to Evaluating the Performance Indicators of Civil Servants, Special Boundary Value Problems for Functional-Differential Equations, Theoretical Mechanics
Scientific Publications: 13 Papers, 21 Theses, 1 Book, 1 Monograph


Name: **Gulnar**
Middle Name: **Rovshan**
Surname: **Mirzayeva**
Birthday: 05.09.1985
Birthplace: Baku, Azerbaijan
Bachelor: Mechanics, Department of Theoretical Mechanics, Faculty of Mechanics and Mathematics, Baku State University, Baku, Azerbaijan, 2006
Master: Mechanics, Department of Theoretical Mechanics, Faculty of Mechanics and Mathematics, Baku State University, Baku, Azerbaijan, 2008
Ph.D.: Mechanics of Oil, Gas and Plasma, Department of Oil, Gas and Plasma, Institute of Mathematics and Mechanics, Baku, Azerbaijan, 2014
Scientific Position: Teacher, Theoretical Mechanics, Department of Control of Intelligent Systems, Academy of Public Administration, Baku State University, Since 2019
Research Interests: Solid Mechanics, Applied Mathematics, Liquid Mechanics, Theoretical Mechanics
Scientific Publications: 40 Papers, 25 Theses


Name: **Alikhan**
Middle Name: **Bayram**
Surname: **Garayev**
Birthday: 01.04.1960
Birthplace: Baku, Azerbaijan
Master: Mechanics, Department of Mechanics, University of Architecture and Construction., Baku, Azerbaijan, 1983
Ph.D.: Mechanics, Department of Mechanics, Azerbaijan University of Architecture and Construction, Baku, Azerbaijan, 1993
Scientific Position: Assoc. Prof., Department of Mechanics, Azerbaijan University of Architecture and Construction, Baku, Azerbaijan, Since 2016
Research Interests: Solid Mechanics, Applied Mathematics, Liquid Mechanics, Theoretical Mechanics
Scientific Publications: 15 Papers, 10 Theses, 2 Books